

Raman Study of the Interface between Hot-Pressed Silica Parts

Alexandre E. Chmel

Fracture Physics Department, Ioffe Physico-Technical Institute, Russian Academy of Sciences,
194021 St. Petersburg, Russia

Andrej N. Smirnov and Victor S. Shashkin

Vavilov State Optical Institute, 193171 St. Petersburg, Russia

We present a Raman spectroscopy study of silica glasses prepared by hot-pressing of gels. Our particular interest is the structure at the interfaces formed during hot-pressing of small parts to obtain large pieces, such as silica tubes for optical-fiber preforms. A specific feature of the interface that distinguishes this layer from the bulk is its fractal structure. The parameters of the fractal units, including their maximum dimensions in real space, are determined by the pre-hot-pressing mechanical processing. We attribute this structure to residual microcracks inherent in the surface layer of polished plates. There are no fractals at the interfaces sintered at temperatures higher than the glass transition temperature.

I. Introduction

MANUFACTURING of monolithic pieces from gel-derived powders by hot-pressing has been known for more than two decades. The optimization of parameters of applied pressure, temperature, and vacuum conditions;^{1,2} the role of the OH⁻ content in the starting gels;² and the mechanism of sintering³ and gel-to-glass conversion⁴ brought about during hot-pressing have received considerable attention. A related issue is the consolidation of small, gel-derived parts to large, monolithic glassware. We have encountered this problem while developing the technology of making silica tubes for optical-fiber preforms. These tubes, 120 mm in length, are obtained by hot-pressing a stack of disks 40 mm in diameter and 10 mm in thickness with subsequent drilling of a longitudinal channel. Our objective is to control the optical quality of the interfaces between the sintered disks. Optical microscopy examination reveals no imperfection in the final products. However, further investigation conducted using Raman spectroscopy provides some evidence for incomplete restoration of the continuous glass structure at the nanostructural level.

II. Samples and Equipment

Samples were prepared from high-purity xerogels obtained by hydrolysis of tetraethyl orthosilicate (TEOS) in a water solution of alkaline at pH 11 and a TEOS/water ratio of ~1:4. The xerogels were dried at 35°C (for 7 d) and 60°C (for 7 d) and then heated at 800°C (for 40 min). The heat-treated product (raw material) was dispersed in a ball mill to a powder with the particle-size distribution shown in Fig. 1. Then the powder was hot-pressed to transparent monolithic disks (primary preforms), 40 mm in diameter and 10 mm in thickness. This primary hot-pressing cycle was performed under a pressure 180 MPa at a temperature of 1150°C.

L. C. Klein—contributing editor

To obtain large samples, the primary preforms were polished, and a stack of uniform disks was hot-pressed again (secondary hot-pressing) under the same or different conditions to a final product.

A particular sample was also made from a couple of fragments of a primary preform. The main crack propagation was initiated from a previously made incision. The fracture surfaces were exactly matched and hot-pressed to a monolithic piece under a compression of 7 MPa at a temperature of 1150°C.

The Raman spectra were excited at 488 nm by an argon laser and recorded with a Raman spectrometer (Model Ramalog 5, Spex Industries, Edison, NJ). The spectra were measured at an angle of 90° to the exciting beam passing through the bulk or along the internal sintering surface (Fig. 2). The laser beam was focused to a spot 100 μm in diameter at the focal length of ~2 mm.

III. Results and Discussion

The Raman spectra are presented in Fig. 3. In the range of the structural bands (at a frequency >200 cm⁻¹), the intensity difference between the spectra of the raw material and the spectra of the hot-pressed products is negligible in the bands at 490 cm⁻¹ and 606 cm⁻¹ belonging to intrinsic defects in the vitreous silica.⁵ The second pressing cycle decreases the defect band intensities to values typical of fused silica (e.g., Refs. 5 and 6), indicating that the process of the structural relaxation is complete under the chosen conditions of the sample preparation.

More-pronounced changes are observed in the low-frequency range, where the boson peak is situated. This feature does not manifest itself in the spectrum of the raw material. After hot-pressing it appears in the spectrum of the primary preform at 40 cm⁻¹; after the second hot-pressing, the boson peak disappears in

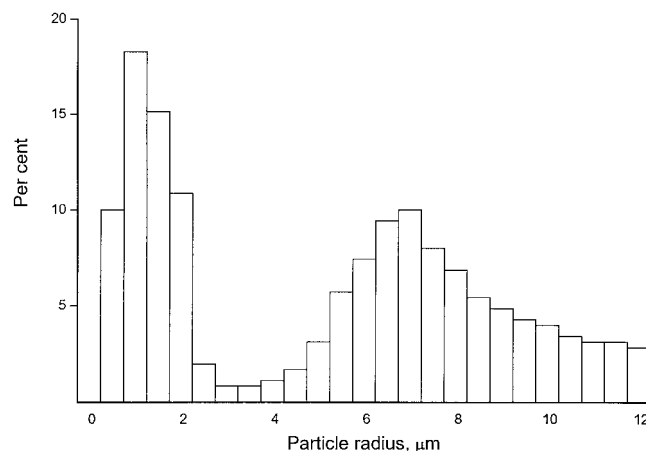


Fig. 1. Particle-size distribution of heat-treated xerogels dispersed in a ball mill.

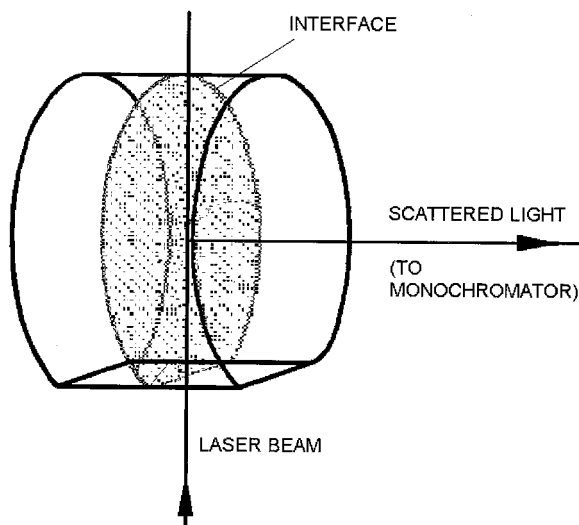


Fig. 2. Scheme of excitation of the Raman spectrum from the interface between hot-pressed pieces. Lower part of the cylindrical sample was cut to facilitate laser beam focusing.

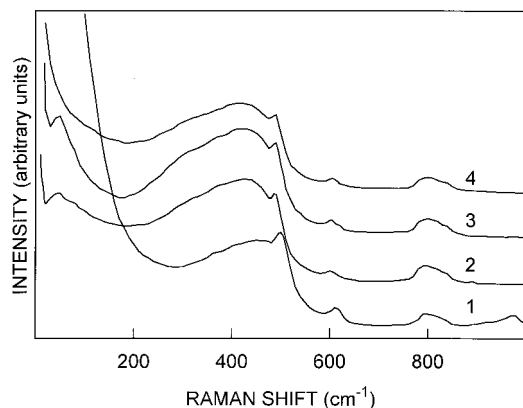


Fig. 3. Raman spectra of the (1) raw material, (2) primary preform, (3) bulk, and (4) interface⁴ of the final product sintered at 1150°C under 180 MPa.

the spectrum of the newly formed interface and appears in the bulk spectrum at 52 cm⁻¹. A strong difference between the samples is observed only in the low-frequency range, where the changes in maximum position and intensity of the boson peak take place.

The position and the intensity of the boson peak reflect the structural ordering (the intermediate-range order) in a material. In particular, the boson peak frequency, ν_B , corresponds to the correlation sphere radius, R_c , as⁷

$$\nu_B \approx 0.7 \frac{v_t}{R_c} \quad (1)$$

where v_t is the transverse sound velocity (in silica, $v_t = 3.8 \times 10^5$ cm s⁻¹). Estimation of R_c for the samples exhibiting the boson peak gives ~ 2.1 nm for the primary preforms and 1.4 nm for the bulk of the final product. At the same time, the intensity of the boson peak is higher in the bulk sample, meaning an increase in the degree of ordering. In other words, as a result of the second hot-pressing cycle, the bulk correlation sphere becomes more compacted and, simultaneously, more ordered.

Now let us consider the cases of the lack of the boson peak in the Raman spectrum. This is observed for raw material (gel) and for sintered interfaces of twice-hot-pressed samples.

According to Ref. 6, the boson peak does not manifest itself in the spectra of "wet" xerogels because of percolation of the Si-OH terminal groups (i.e., resulting from dynamic isolation of structural units). The spectrum of the raw material shown in Fig. 3 is similar.

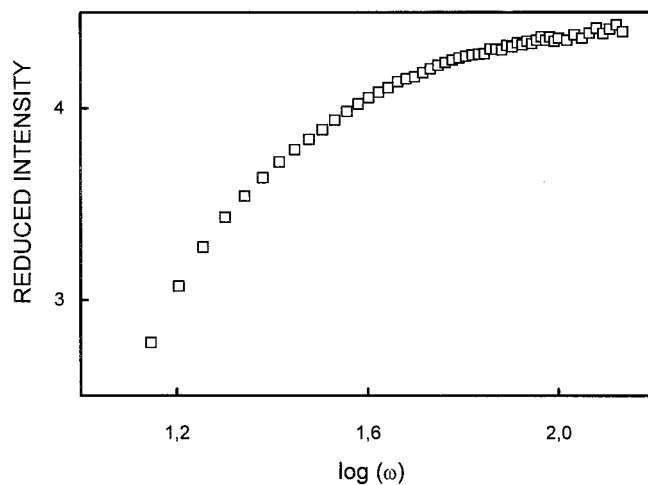


Fig. 4. Low-frequency Raman spectrum of the raw-material sample (for original spectrum, see curve 1 in Fig. 3).

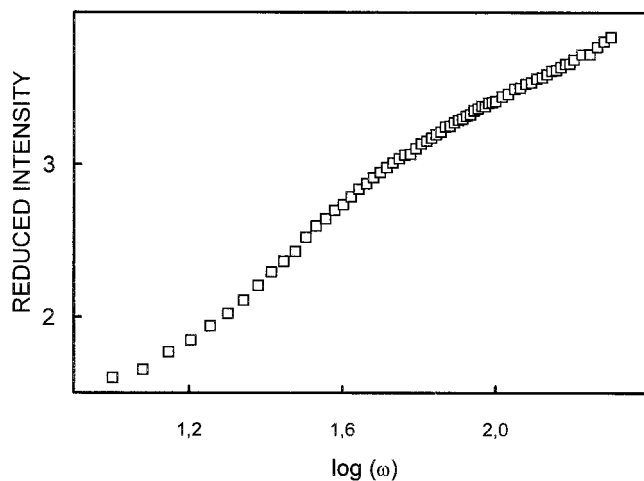


Fig. 5. Low-frequency Raman spectrum of the primary preform (for original spectrum, see curve 2 in Fig. 3).

In contrast, the absence of the boson peak in the spectrum of the interface in the final sample seems surprising. Applying again the concept of percolation,⁶ the decay of the structural correlation can be ascribed to many chemical bonds that are ruptured in the region of newly formed interface, i.e., in the mechanically disturbed surface layer. At the same time, the low-frequency Raman spectrum of the interface reveals fractal structure formation.

The fractal geometry of the fracture surface in glass-ceramics is reported in Ref. 8. Polishing of the primary preform produces a damaged layer consisting of many microcracks. Under this condition, i.e., when fractal ordering changes for randomly correlated structure, the boson peak disappears.⁹ The expression for Raman intensity $I(\omega)$ of the light scattered by vibrational excitations of fractal units is^{10,11}

$$\frac{I(\omega)}{n(\omega) + 1} \propto \omega^{3-\tilde{d}} \quad (2)$$

where $n(\omega) = 1/[\exp(h\omega/k_B T) - 1]$ is the Bose factor and \tilde{d} the so-called fracton dimensionality. The difference between \tilde{d} and the "ordinary" fractal dimensionality is that the latter parameter describes the geometry of structure and the former parameter is related to the geometry of vibrations.

To simplify, the left-hand side of Eq. (4) can be designated as $I_{\text{red}}(\omega)$. Then we have

$$I_{\text{red}}(\omega) \propto \omega^{3-\tilde{d}} \quad (3)$$

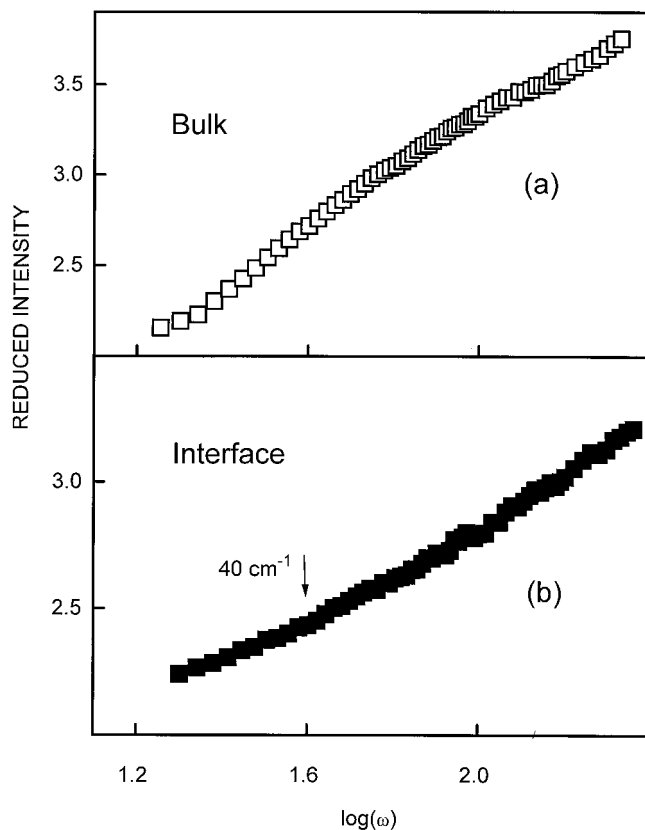


Fig. 6. Low-frequency Raman spectra of the (a) bulk and (b) interface of a couple of polished preforms sintered at 1150°C under 180 MPa. Here, and in Figs. 7 and 8, an arrow in (b) indicates the cutoff frequency (for original spectra, see curves 3 and 4 in Fig. 3).

In other words, in log–log coordinates, $\log I_{\text{red}}(\omega)$ versus $\log \omega$, the plotted frequency dependence for the intensity of the light scattered on fractals should be a straight line with a slope $3 - \bar{d}$. There is no boson peak in an ordered structure.

To establish why the boson peak is absent, we have replotted the low-frequency portions of the spectra in log–log scale (Figs. 4 to 6). Figure 4 shows that the spectra of the bulks of all the samples represent complicated dependencies that do not follow the relation.³ On the contrary, the spectrum of the interface transforms to a linear plot in the range 40–220 cm^{-1} , thus pointing out the presence of the fractal structure in the sintered layer.

The crack size confines the geometric (Euclidean) dimension of the fractal units; in turn, the vibration localized at the largest fractal unit has the lowest frequency, ω_{cutoff} . Therefore, the linear dependence³ is limited at the frequency range. We can roughly estimate the maximum real dimension of the fractal units, D_f , from the Raman data. In a crude approximation, the parameters ω_{cutoff} and D_f , are related as

$$D_f \approx 2\pi \frac{v_t}{\omega_{\text{cutoff}}} \quad (4)$$

Substituting $\omega_{\text{cutoff}} = 40 \text{ cm}^{-1}$ (Fig. 6(b)) into Eq. (4), we obtain $D_f \approx 3.5 \text{ nm}$.

To modify the actual fractal-size distribution and to find a correspondent response in the Raman spectrum, two conjugated fracture surfaces produced by breaking a primary preform are exactly matched and hot-pressed under very low compression (7 MPa). We would expect that the size of unhealed islands at the sintered macroscopic crack would have less influence on the fractal unit dimensions in real space than the submicrocracks in the polished layer. The result demonstrated in Fig. 7 confirms this idea. The range of linearity is expanded from the low-frequency side from 40 to 18 cm^{-1} . The $\omega_{\text{cutoff}} = 18 \text{ cm}^{-1}$ corresponds to

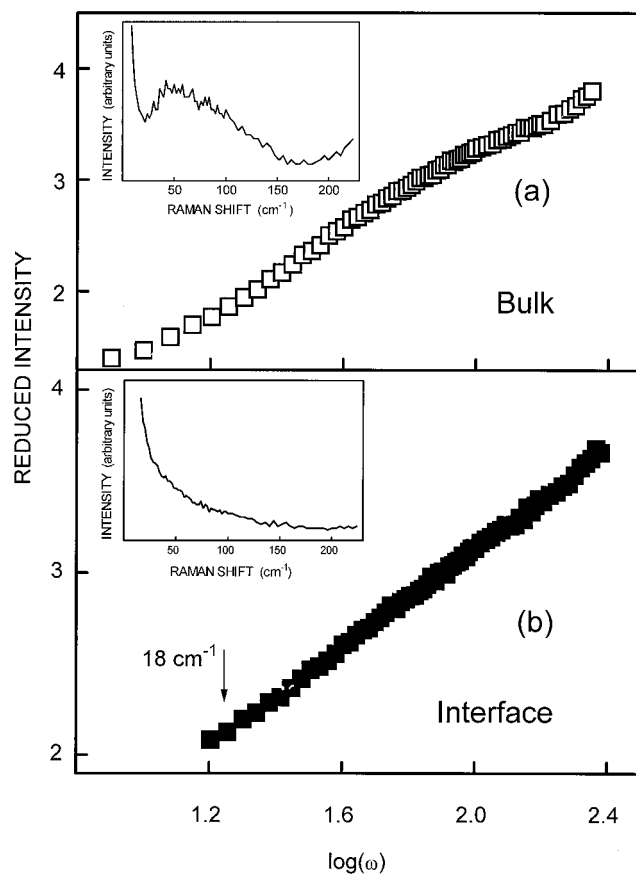


Fig. 7. Low-frequency Raman spectra of the (a) bulk and (b) interface of a couple of matched fracture surfaces sintered at 1150°C under 7 MPa. Here, and in Figs. 8 and 9, the insets correspond to original spectra.

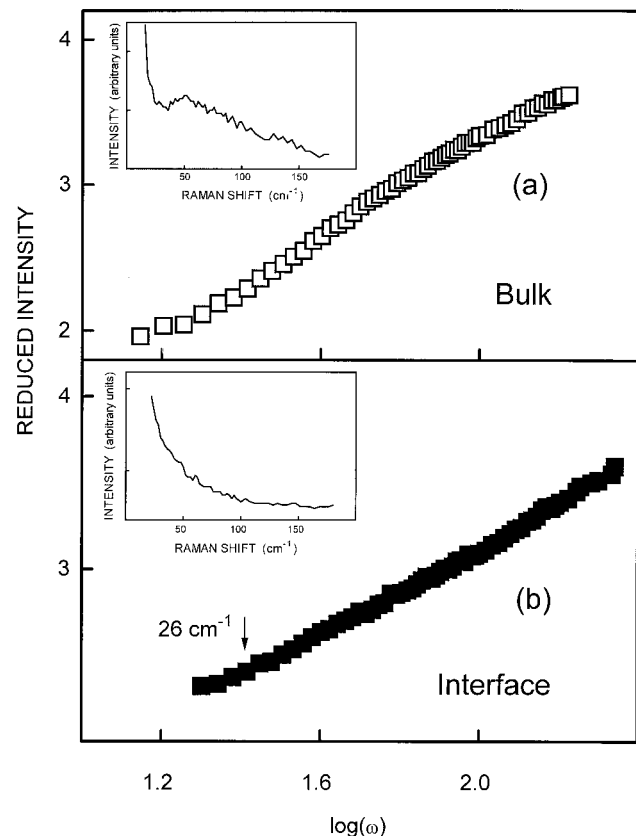


Fig. 8. Reduced Raman spectra of the (a) bulk and (b) interface of the polished sample hot-pressed at 1150°C under 7 MPa.

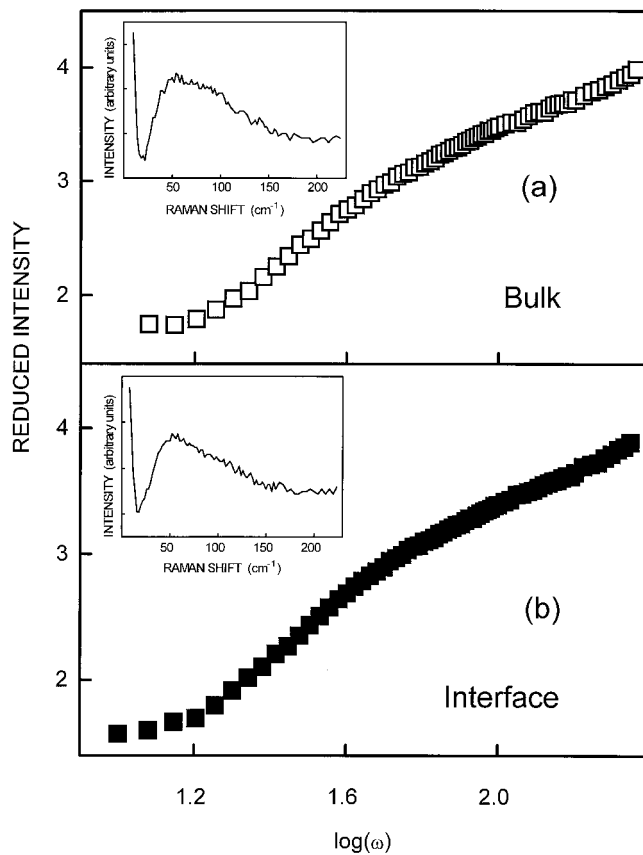


Fig. 9. Reduced Raman spectra of the (a) bulk and (b) interface of the polished sample hot-pressed at 1200°C under 180 MPa.

$D_f \approx 7.5$ nm, which is two times larger than the case of the polished disks.

When the polished disks are hot-pressed under 7 MPa, the cutoff frequency appears at 26 cm^{-1} (Fig. 8), thus giving $D_f \approx 5.0$ nm, despite the 3.5 nm obtained as the result of hot-pressing under 180 MPa. The increase of the size of residual cracks under decreased pressure seems reasonable.

Complete annihilation of microcracks is achieved by increasing the hot-pressing temperature above the glass transition temperature ($T_g \approx 1160^\circ\text{C}$). The results are shown in Fig. 9, which show

ordinary Raman spectra of quartz glass with the boson peak situated at its usual position, 60 cm^{-1} . Consequently, the enhanced mobility of the structural units at $T > T_g$ removes the traces of the fractal structure at the interface, i.e., in fact, obscures the interface itself.

IV. Conclusion

This work has been designed to obtain large glass objects by hot-pressing a stack of small, gel-derived disks. The interface between sintered parts is a region of local heterogeneity. Low-frequency Raman spectroscopy is used to monitor the structural evolution at all stages of the process. The raw material (wet xerogel) exhibits only Rayleigh scattering in this spectral range. The appearance of the boson peak after heat treatment demonstrates the gel-to-glass transition. However, this intermediate-range order decays as a result of mechanical polishing. The layers disturbed by microcracks exhibit a particular type of ordered structure that is fractal. In turn, the fractal order disappears when the final hot-pressing cycle is conducted at a temperature above the glass transition temperature.

References

- ¹M. Decottignies, J. Phalippou, and J. Zarzycki, "Synthesis of Glasses by Hot-Pressing of Gels," *J. Mater. Sci.*, **13**, 2605–13 (1978).
- ²K. Yanagisawa, M. Nishioka, and K. Ioku, "Low-Temperature Sintering of Spherical Silica Powder by Hydrothermal Hot-Pressing" *J. Ceram. Soc. Jpn., Int. Ed.*, **99**, 58–61 (1991).
- ³R. M. Spriggs and S. K. Dutta, "Mechanisms of Sintering During Hot-Pressing and Recent Technological Advances," *Mater. Sci. Res.*, **6**, 369–94 (1973).
- ⁴C. J. Brinker and W. G. Scherer, *Sol-Gel Science: The Physics and Chemistry of Sol-Gel Processing*; pp. 716–17. Academic Press, San Diego, CA, 1990.
- ⁵A. E. Geissberger and F. L. Galeener, "Raman Studies of Vitreous SiO_2 versus Fictive Temperature," *Phys. Rev. B: Condens. Matter*, **28**, 3266–71 (1983).
- ⁶G. Mariotto, M. Montagna, G. Viliiani, R. Camprostrini, and G. Carturan, "Low-Frequency Raman Spectra of Thermally Treated Silica Gels: Observation of Phonon-Fracton Crossover," *J. Phys. C: Solid State Phys.*, **21**, L797–L801 (1988).
- ⁷A. J. Martin and W. Brenig, "Model for Brillouin Scattering in Amorphous Solids," *Phys. Status Solidi B*, **64**, 163–72 (1974).
- ⁸J. J. Mecholsky, D. E. Passoja, and K. S. Feinberg-Ringel, "Quantitative Analysis of Brittle Surfaces Using Fractal Geometry," *J. Am. Ceram. Soc.*, **72**, 60–65 (1989).
- ⁹S. Alexander, C. Laermans, R. Orbach, and H. M. Rosenberg, "Fracton Interpretation of Vibrational Properties of Cross-Linked Polymers, Glasses, and Irradiated Quartz," *Phys. Rev. B: Condens. Matter*, **28**, 4615–19 (1983).
- ¹⁰A. Boukenter, B. Champagnon, E. Duval, J. Dumas, J. F. Quinson, and J. Serughetti, "Low-Frequency Raman Scattering from Fractal Vibrational Modes in a Silica Glass," *Phys. Rev. Lett.*, **57**, 2391–94 (1986).
- ¹¹A. Boukenter, B. Champagnon, E. Duval, and J. L. Rousset, "Low-Frequency Raman Scattering from Disordered or Heterogeneous Materials," *Philos. Mag. B*, **59** [1] 125–31 (1989). □